Petroleum and Coal

Article **Open Access**

Improving H-Oil Ebullated Bed Vacuum Residue Hydrocracking Performance By The Use Of Molecularly Dispersed HCAT® Catalyst

Dicho Stratiev[1], Ivelina Shishkova[1], Georgy Argirov[1], Vasil Yankov[1], David Mountainland[2], Brett Silverman[2], Vesislava Toteva[3]

[1] *LUKOIL Neftohim Burgas, 8104 Burgas, Bulgaria*
[2] *HTI 1501 New York Avenue Lawrenceville, NJ 08648, USA*
[3] *University of Chemical Technology and Metallurgy, 8 "Kl Ohridski" boul, 1756 Sofia, Bulgaria*

Received February 15, 2021; Accepted May 20, 2021

Abstract

The LUKOIL Neftohim Burgas (LNB) refinery, which features the H-Oil® ebullated bed vacuum residue hydrocracking in its petroleum refining processing scheme, employs HCAT, HTI's proprietary dispersed nano-size catalyst technology, to boost the H-Oil performance. The positive results from HTI's pilot plant hydrocracking experiments were confirmed at the commercial LNB H-Oil hydrocracker, registering a conversion increase of about eight per cent without penalizing the sediment formation rate. The increased H-Oil vacuum residue conversion led to increased density, viscosity, and softening point of the unconverted hydrocracked vacuum residue which require further optimization of the utilization of this product. The increased H-Oil vacuum residue conversion as a result from the use of HCAT did not have an impact on the performance of the fluid catalytic cracking unit that processes a blend of straight run vacuum gas oil (VGO) and H-Oil VGO.

Keywords: *Ebullated bed hydrocracking; Vacuum residue, Molecularly dispersed HCAT catalyst, Conversion, Product quality.*

1. Introduction

The main limitation for conversion increase in the ebullated bed vacuum residue hydrocracking is the formation of sediments [1-9]. The sediments increase exponentially when reaction temperature is raised [5, 10-11] due to the fact that the rates of thermal cracking reactions increase more rapidly than the hydrogen addition counterparts [12]. Thus, hydrogen transfer limitations occur, which can lead to the growth of aromatic structures in the asphaltenes, making them more prone to precipitate once these compounds leave the reactor zone [12]. The use of molecularly dispersed catalyst from metal–organic precursors such as iron pentacarbonyl or molybdenum 2-ethylhexanoate formed in situ [13] was reported to improve the commercial ebullated bed vacuum residue hydrocracking performance [14-15]. This molecularly dispersed catalyst is known as HCAT [16]. The homogenous HCAT catalyst is mixed throughout the heavy oil feedstock and is dispersed using HTI's proprietary mixing system. Maximal dispersion of the HCAT results in a highly active nano-scale catalyst. HCAT addition to the ebullated bed increases conversion of the asphaltenes which results in decreased sediment formation and fouling within all critical equipment of the process. [13]. The application of the highly dispersed catalysts in the hydroprocessing of heavy residues favors the rapid uptake of hydrogen and deactivates the intermediate free radical moieties in the liquid phase, thereby suppressing coke formation, enabling the increase in total conversion, and enhancing quality of liquid product [13]. The nano-size unsupported dispersed catalysts can be used along with the conventional supported catalysts and improve the performance of the ebullated bed vacuum residue hydrocracking by retarding the process of sediment formation [15, 17]. The LNB refinery decided to implement the HCAT Technology as a tool to optimize H-Oil performance after successfully testing the process at the HTI Pilot Plant. The pilot studies utilized a true

ebullated bed pilot unit to process LNB's H-Oil feedstock along with LNB's Ni-Mo supported catalyst and HCAT. The aim of this study was to discuss the results obtained in a laboratory pilot vacuum residual oil (VRO) hydrocracking plant, and at the commercial LNB H-Oil VRO hydrocracker before and after the use of the HCAT catalyst.

2. Experimental

The commercial hydrocracking demonstration was performed at the LNB H-Oil ebullated bed VRO hydrocracking unit. A simplified process diagram of the LNB EBVR H-Oil hydrocracker and the conditions at which it operates are presented in [18]. The reaction temperature. liquid hourly space velocity (LHSV), the level of sediments in the LNB H-Oil atmospheric tower bottom (ATB) product, and the properties of the H-Oil VTB's obtained during hydrocracking of the feed streams, whose properties are shown in Table 1 are summarized in Table 2. The catalyst employed in this study was a commercial Ni-Mo low sediment catalyst.

Table 1. Data from the pilot plant experiments with and without using the nano-size catalyst HCAT

Run	Feed	1	2	3	4	5
Nano-size catalyst		No HCAT	HCAT	HCAT	HCAT	HCAT
LHSV, h-1		Base	Base	Base	Base	Base
WABT, °C		Base	Base	Base+6	Base+10	Base+14
H-Oil Net Conversion (540°C+), wt.%		64.2	65.2	68.1	74.4	80.0
ATB sediment content, wt.%	0	0.33	0.07	0.09	0.15	0.27
VTB C7 asp. content, wt.%	7.3	11.5	9.0	11.0	11.7	16.3
VTB MCR content, wt.%	18	25.5	25.5	27.0	28.0	34.0
VTB sulphur content, wt.%	3.86	2.08	1.75	1.84	1.86	1.90
VTB viscosity at 150°C, cP		60.0	60.0	65.0	70.0	130.0
Gas yield, wt.% (C_1-C_4)		3.70	3.70	4.30	5.00	5.90
Naphtha yield, wt.% (C_5-146°C)		5.7	5.6	6.7	7.8	9.7
Diesel yield, wt.% (146-362°C)		25.7	26.3	28.5	32.4	36.6
VGO yield, wt.% (362-540°C)		32.9	33.1	31.7	31.6	29.3
VTB yield, wt.% (>540°C)		29.6	29.4	26.4	21.1	16.3

Table 2. Correlation matrix of the parameters from the pilot plant experimental data shown in Table 1

	WABT	*Conv.*	*TSE*	*Asp*	*MCR*	*Sul.*	*VIS*	*Gas*	*Naphtha*	*Diesel*	*VGO*	*VTB*
WABT	1.00											
Conv.	**0.98**	1.00										
TSE	0.05	-0.14	1.00									
Asp	**0.82**	**0.85**	0.02	1.00								
MCR	**0.90**	**0.94**	-0.06	**0.94**	1.00							
Sul.	-0.11	-0.11	0.10	0.33	-0.01	1.00						
VIS	**0.81**	0.88	-0.10	**0.94**	**0.99**	0.03	1.00					
Gas	**0.98**	**1.00**	-0.06	0.88	0.95	-0.07	0.89	1.00				
Naphtha	**0.98**	**0.99**	-0.05	0.90	0.97	-0.04	0.92	1.00	1.00			
Diesel	**0.98**	**1.00**	-0.12	0.86	0.95	-0.10	0.89	1.00	0.99	1.00		
VGO	**-0.94**	**-0.94**	-0.11	-0.93	-0.98	0.02	-0.94	-0.97	-0.98	-0.95	1.00	
VTB	**-0.98**	**-1.00**	0.12	-0.86	-0.94	0.07	-0.88	-1.00	-0.99	-1.00	0.95	1.00

The vacuum residue 540°C+ conversion was estimated by the equation:

$$\text{Conversion } (\%) = \frac{EBRHCFeed_{540°C+} - EBRHC\,\text{Pr}oduct_{540°C+}}{EBRHCFeed_{540°C+}} \times 100 \qquad \text{eq. (1)}$$

where: $EBRHCFeed_{540°C+}$ = mass flow rate of the EBVRHC feed fraction boiling above 540°C, determined by high temperature simulated distillation (method ASTM D 7169) of the feed and multiplied by the mass flow rate of the feed in t/h; $EBRHCProduct_{540°C+}$ = mass flow rate of the EBVRHC product fraction boiling above 540°C, determined by high temperature simulated distillation (method ASTM D 7169) of the liquid product multiplied by the flow rate of the liquid product in t/h.

The SARA fraction conversions were calculated by the equation:

$$SARA\ fraction\ conversion.\,\% = \frac{\text{Feed SARA} - \text{Product SARA}}{\text{Feed SARA}} * 100 \qquad \text{eq. (2)}$$

where: Feed SARA = SARA fraction (saturates, aromatics (naphtheno-aromatics), resins (polar aromatics), asphaltenes) content in the vacuum residual oil feed, % multiplied by the feed rate in t/h;

Product SARA = SARA fraction (saturates, aromatics (naphtheno-aromatics), resins (polar aromatics), asphaltenes) content in the hydrocracked vacuum residual oil (H-Oil VTB) product, % multiplied by the H-Oil vacuum tower bottom (VTB) product flow rate in t/h.

The total existent sediment content (TSE) of the residual oils studied in this work was measured in accordance with the procedure IP 375 [19]. The total sediment potential (TSP) of the residual oils studied in this work was measured in accordance with the procedure IP 390 [20]. The precision of the measurement of TSE, and TSP expressed by the repeatability and reproducibility is summarized below:

$r = 0.089\sqrt{HFT_{Result}}$ Repeatability eq.(3)

$R = 0.294\sqrt{HFT_{Result}}$ Reproducibility eq.(4)

The process flow diagram of the ebullated-bed pilot plant used to perform the laboratory VRO hydrocracking experiments with and without HCAT catalyst is presented in Figure 1.

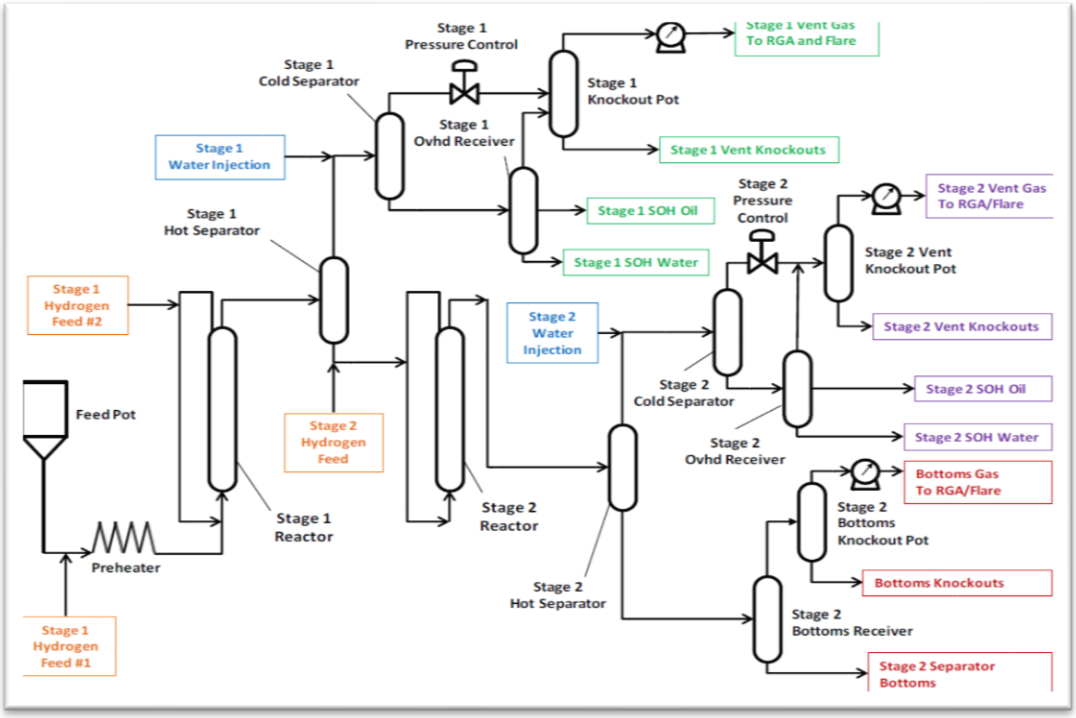

Figure 1. Process flow diagram of the ebullated-bed pilot plant to investigate the effect of using the HCAT catalyst during processing the VRO blend 70% Urals/ 30% Basrah Light

3. Results and discussion

The laboratory pilot plant VRO hydrocracking experiments with and without using the HCAT catalyst are summarized in Table 1. The data from Table 1 was used to make the graphs in Figure 2.

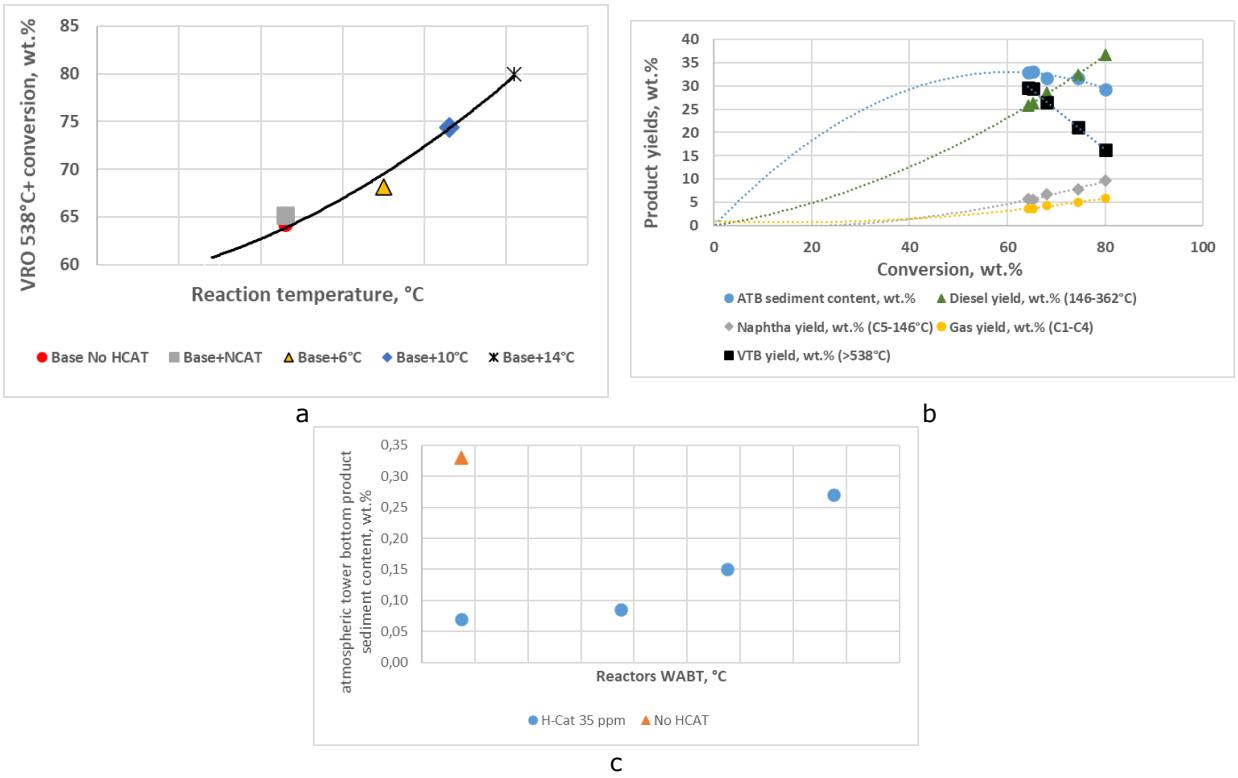

Figure 2. Conversion dependence on reaction temperature (a) and product yields selectivity curves (b), and ATB sediment content vs WABT (c)

The data in Table 1, and Figure 2 shows that the employment of HCAT in a base concentration of the feed, significantly decreases the level of sediments in the ATB product (from 0.33 down to 0.07% at constant operating conditions). This allowed a reaction temperature increase by 14°C and consequently conversion level raising by 15% without reaching the ATB sediment level obtained without using the dispersed HCAT catalyst. The product selectivity curves shown in Figure 2 b indicates the typical distribution of the primary unstable product (VGO) yield and of the primary + secondary stable product (gas, naphtha, diesel) yields as a function of conversion as already discussed in our earlier research [21]. It is evident from the data in Figure 3 b that the VGO yield goes through a maximum at about 60% and then falls, while the yields of gas, naphtha and diesel continually increase with conversion raise. The VTB yield linearly decreases with the increment of conversion. In order to better follow the relations between the properties of the VTB product (538°C) from the pilot plant experiments and the relations of all parameters shown in Table 1 a correlation matrix was made. It is presented as Table 2. It is evident from the data in Table 2 that the VTB asphaltene content correlates with the VTB microcarbon residue (MCR) content, and with the VTB viscosity. The data in Table 1 indicate that with the increase of reaction temperature, and consequently increase of conversion the asphaltene content, the MCR content, and the viscosity of the VTB goes up. With the hydrocracking reaction progress the unconverted hydrocracked vacuum residual oil becomes more hydrogen deficient that is reflected by a higher MCR content, and higher viscosity

Similar relation between the aromaticity (expressed by density, and/or hydrogen content) and the viscosity was also found out for the vacuum gas oil fluid catalytic cracking (FCC) main column bottom slurry oil (FCC SLO) product and the viscosity of the FCC SLO [22].

Table 3. Summary of the data from the commercial application of HCAT at the LNB H-Oil ebullated bed vacuum residue hydrocracker

Date	5.2. 2020	6.2. 2020	7.2. 2020	12.2. 2020	13.2. 2020	14.2. 2020	15.2. 2020	1.3. 2020	2.3. 2020	3.3. 2020	4.3. 2020	5.3. 2020	6.3. 2020	7.3. 2020	8.3. 2020	9.3. 2020
HCAT (Dosage)	No HCAT	No HCAT	No HCAT	HCAT (High)	HCAT (High)	HCAT (High)	HCAT (High)	HCAT (Mid)	HCAT (Low)	HCAT (Low)	HCAT (Low)	HCAT (Low)	HCAT (Low)	HCAT (Low)	HCAT (Low)	HCAT (High)
LHSV, h^{-1}	Base	Base	Base	Base	Base	Base	Base	0.9*Base	0.9*Base	0.9*Base	0.9*Base	0.9*Base	0.9*Base	0.9*Base	0.9*Base	0.9*Base
H-Oil WABT,°C	Base	Base	Base	Base+5.5	Base+6	Base+7	Base+6	Base+6	Base+6	Base+6	Base+6	Base+6	Base+6	Base+6	Base+6	Base+6
H-Oil ATB TSE, wt.%	0.12	0.10	0.22	0.10	0.09	0.07	0.12	0.07	0.08	0.08	0.08	0.07	0.07	0.06	0.06	0.05
PBFO TSP, wt.%	0.07	0.13	0.17	0.18	0.14	0.11	0.13	0.13	0.10	0.10	0.08	0.10	0.08	0.09	0.10	0.13
H-Oil Net Conv.,%	72.2	74.1	72.7	78.5	79.0	79.7	80.8	81.5	80.6	80.7	80.5	80.7	80.9	79.0	80.8	80.3
H-Oil Conv. as is, wt.%	72.4	72.8	72.4	77.9	78.6	79.0	79.3	82.67	82.28	82.53	81.94	81.44	80.76	80.15	80.86	80.81
Gas yield, wt.%	7.39	7.40	7.40	8.41	8.38	8.83	9.30	9.23	9.34	9.29	9.74	9.69	9.01	9.28	9.05	9.35
Naphtha yield, wt.%	6.6	7.0	7.1	7.5	7.7	8.4	8.9	9.5	8.9	8.5	8.8	9.0	8.7	8.3	8.9	8.9
Diesel yield, wt.%	29.6	30.4	31.0	33.3	34.0	34.6	34.2	35.6	35.2	35.2	34.4	33.7	34.5	34.7	35.0	34.6
VGO yield, wt.%	32.6	31.7	30.5	32.5	32.3	30.9	30.8	32.6	33.1	33.8	33.3	33.5	32.8	32.1	32.2	32.3
VTB yield, wt.%	24.6	23.5	23.7	18.5	17.8	17.4	17.2	14.0	14.4	14.2	14.7	15.1	15.8	16.7	15.8	15.9
FCC SLO in H-Oil Feed, wt.%	7.8	7.8	7.8	7.7	7.8	7.8	8.3	11.4	11.7	12.0	12.0	12.0	12.0	12.0	13.9	14.2
Predicted by LNB Model H-Oil Conversion, wt.%	74.7	74.8	74.7	79.9	80.5	81.4	81.5	82.6	82.5	82.5	82.6	82.6	82.5	82.4	82.6	82.5

Table 4. Correlation matrix of commercial data for the application of HCAT at the LNB H-Oil employing the data from Table 3

	LHSV	*WABT*	*ATB TSE*	*TSP*	*Net Conv.*	*H-Oil Conv.*	*Gas yield*	*Naphtha yield*	*Diesel yield*	*VGO yield*	*VTB yield*	*FCC SLO in H-Oil Feed*	*Predicted Conv.*
LHSV	1.00												
WABT	-0.56	1.00											
ATB TSE	0.59	-0.71	1.00										
TSP	0.52	-0.16	0.48	1.00									
Net Conv.	-0.71	**0.95**	-0.72	-0.20	1.00								
H-Oil Conv.	-0.82	**0.91**	-0.72	-0.31	**0.96**	1.00							
Gas yield	-0.82	**0.88**	-0.67	-0.36	**0.93**	0.95	1.00						
Naphtha yield	-0.84	**0.82**	-0.62	-0.28	**0.93**	0.92	0.93	1.00					
Diesel yield	-0.70	**0.94**	-0.65	-0.15	**0.95**	0.95	0.88	0.89	1.00				
VGO yield	-0.58	0.31	-0.54	-0.49	0.39	0.55	0.46	0.32	0.31	1.00			
VTB yield	0.80	**-0.92**	0.70	0.27	**-0.97**	-1.00	**-0.95**	**-0.92**	**-0.96**	-0.52	1.00		
FCC SLO in H-Oil Feed	-0.94	0.51	-0.63	-0.46	0.63	0.73	0.72	0.73	0.63	0.55	-0.71	1.00	
Predicted Conv.	-0.76	0.96	-0.75	-0.29	**0.98**	**0.98**	**0.95**	**0.91**	**0.96**	0.44	**-0.98**	0.71	1.00

**Note: The marked in bold figures concern statistically meaningful correlation (R≥0.75; weak correlation for 0.75<R<0.85; medium correlation for 0.85<R<0.95; strong correlation for R≥0.95)*

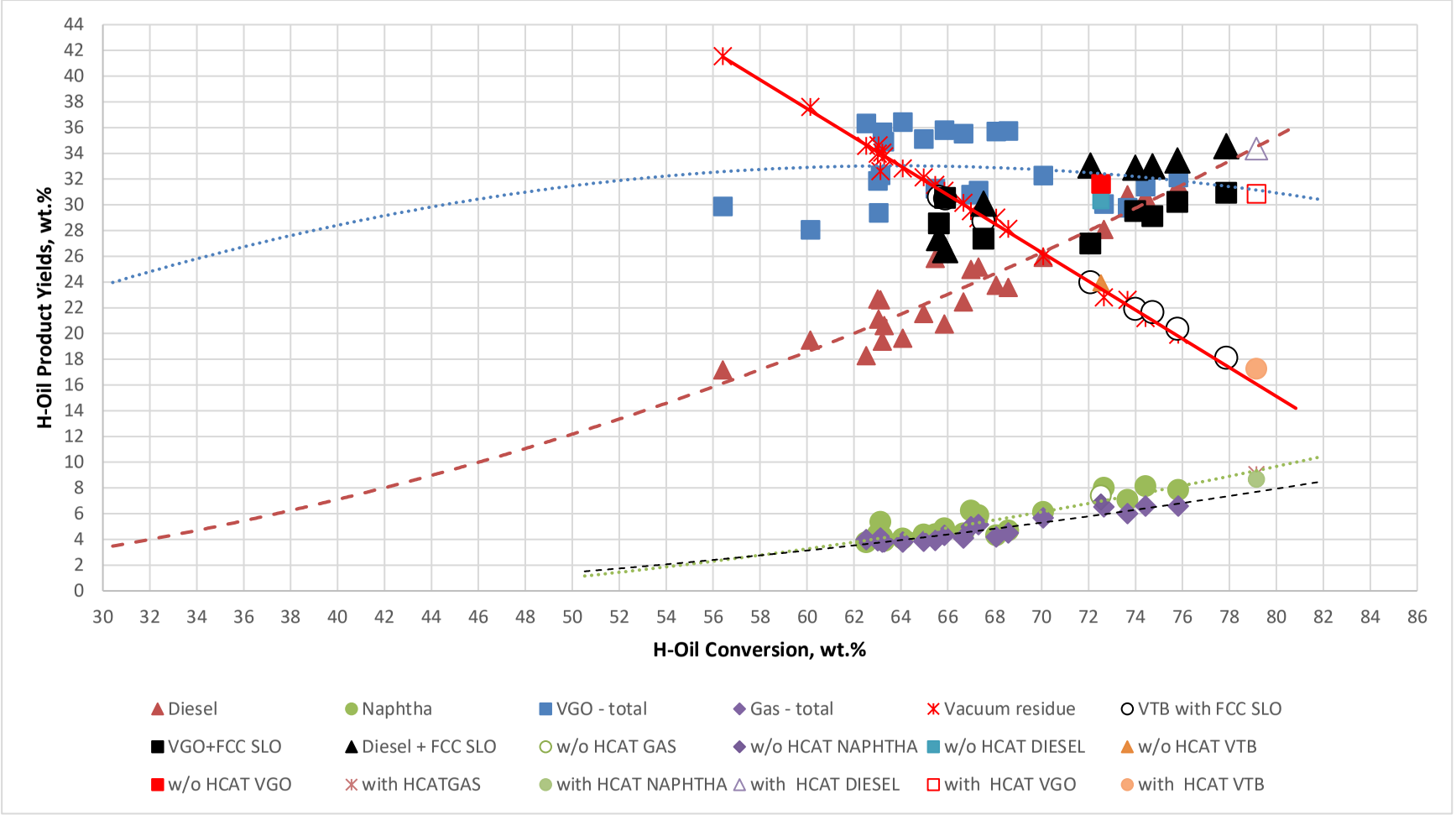

Figure 3. Selectivity curves of the product yields as a function of conversion in the commercial LNB H-Oil hydrocracker

Table 5. Data about the properties of the LNB H-Oil hydrocracker feed and products with and without using HCAT

Nr	Sample	Date	HCAT use	D_{15}, g/cm^3	IBP	T_{10}	T_{30}	T_{50}	T_{70}	T_{90}	T_{95}	FBP	CCR, wt.%	C_5 asp., wt.%	C_7 asp., wt.%	C_5 asp. D_{15}, g/cm3	C_7 asp. D_{15}, g/cm3	Sat.,%	Aro.,%	Res.,%	Asp.,%	Sulphur, wt.%
1	H-Oil Feed	6.2.2020	No HCAT	1.031	304	473	575	621	659	710	739	820	17.2	19.2	14.6	1.156	1.179	15.8	65.0	4.7	14.6	3.74
2	H-Oil Feed	13.2.2020	with HCAT	1.028	313	473	571	616	654	701	715	759	17.1	19.8	12.8	1.182	1.201	16.4	63.9	6.9	12.8	3.09
3	H-Oil Feed	15.2.2020	with HCAT	1.019	233	456	569	615	653	702	718	780	17.1	19.3	13.1	1.163	1.175	18.4	62.3	6.2	13.1	2.84
4	ATB	6.2.2020	No HCAT	0.993	304	391	458	516	573	653	688	777			10.5		1.264	30.7	50.8	8.0	10.5	1.23
5	ATB	13.2.2020	with HCAT	0.992	280	379	442	498	558	642	680	771			9.16		1.285	30.9	52.0	8.0	9.2	1.08
6	ATB	15.2.2020	with HCAT	0.997	299	383	446	501	561	645	684	774			10.59		1.264	29.3	52.1	8.0	10.6	1.15
7	VTB	6.2.2020	No HCAT	1.046	350	529	573	604	642	697	718	819	26.2	30.2	18.4	1.220	1.279	21.8	47.9	11.8	18.4	1.80
8	VTB	13.2.2020	with HCAT	1.063	349	527	573	604	641	698	720	847	28.8	32.2	22.1	1.237	1.287	20.0	47.8	10.1	22.1	0.94
9	VTB	15.2.2020	with HCAT	1.069	382	528	572	603	640	695	715	800	24.2	35.1	24.7	1.235	1.251	19.5	45.4	10.4	24.7	1.58
10	Diesel	6.2.2020	No HCAT	0.856	118	174	227	271	314	356	370	392										0.17
11	Diesel	13.2.2020	with HCAT	0.849	107	166	216	261	303	347	362	384										0.15
12	Diesel	15.2.2020	with HCAT	0.851	112	172	218	262	304	350	365	389										0.16
13	HAGO	6.2.2020	No HCAT	0.936	247	342	381	402	425	467	491	552										0.55
14	HAGO	13.2.2020	with HCAT	0.936	245	338	377	398	420	459	482	543										0.52
15	HAGO	15.2.2020	with HCAT	0.938	247	339	379	400	422	462	485	546										0.56
16	LVGO	6.2.2020	No HCAT	0.953	266	344	385	413	442	495	520	570	0.01									0.68
17	LVGO	13.2.2020	with HCAT	0.953	265	341	383	411	441	493	519	572	0.03									0.65
18	LVGO	15.2.2020	with HCAT	0.954	266	341	382	410	439	491	517	570	0.00									0.69
19	HVGO	6.2.2020	No HCAT	0.963	361	421	460	488	514	548	562	599	0.17									0.88
20	HVGO	13.2.2020	with HCAT	0.964	361	421	460	488	514	548	564	602	0.78									0.87
21	HVGO	15.2.2020	with HCAT	0.968	360	420	458	486	513	546	561	595	0.50									0.92
22	VTB	6.3.2020	with HCAT	1.044	400	540	583	614	650	705	735	852										1.65
23	HAGO	9.3.2020	with HCAT	0.950	266	343	377	397	418	455	476	531										0.50
24	LVGO	9.3.2020	with HCAT	0.971	273	343	384	414	444	493	517	566										0.62
25	HVGO	9.3.2020	with HCAT	0.9849	362	426	463	491	516	548	562	595										0.86

Table 3 summarizes the commercial results with and without using HCAT in the LNB H-Oil ebullated bed VRO hydrocracking unit. A correlation matrix (Table 4) was made to follow the relations of the parameters of the commercial LNB H-Oil VRO hydrocracker, summarized in Table 3. The data in Table 3 indicates that the atmospheric tower bottom (ATB) total sediment existent (Shell hot filtration test, IP 375) did not increase regardless of weight average bed temperature (WABT) heightening from Base to Base+7°C with the use of HCAT. There was no change in the total sediment potential (TSP = sediment content of the hot filtration test after thermal aging, IP 390) of the partially blended fuel oil (PBFO), which is obtained by addition of FCC heavy cycle oil (HCO) to the H-Oil vacuum tower bottom (VTB) product. This confirmed our conclusion made in our recent research [23] that the property TSP of the heavy fuel oil produced on the base of the H-Oil residual oils is difficult to control. Similar to the results from the hydrocracking experiments in the laboratory unit (Table 2) the commercial LNB H-Oil hydrocracker also showed a strong relation of the net conversion to the reactors WABT (R=0.95). The relation of the reactors WABT to the product yields in the commercial LNB H-Oil hydrocracker is not so strong as that registered in the laboratory pilot plant. This can be explained with the imperfect fractionation of the products from the reaction mixture in the commercial H-Oil VRO hydrocracker. This is a testimony that an improvement in the extraction extent of the higher value light products from the reaction mixture in the commercial H-Oil VRO hydrocracker can be made. Figure 3 shows a graph of selectivity curves of the product yields as a function of conversion in the commercial LNB H-Oil hydrocracker. These selectivity curves are not distinctly different from those observed in the laboratory pilot plant (Figure 2 b).

However, the data in Figure 3 are characterized with more scatter supporting the statement that an improvement in the extraction extent of the higher value light products from the reaction mixture in the commercial H-Oil VRO hydrocracker can be achieved. As a whole, it could be concluded that the employment of the HCAT Technology at the commercial H-Oil VRO hydrocracker allowed increase of WABT by 7°C that led to conversion raise of 6.7% without augmentation of the ATB TSE.

Table 5 presents data about the properties of the LNB H-Oil hydrocracker feed and products with and without using HCAT. The data in Table 5 indicates that the increased WABT in the LNB H-Oil hydrocracking reactors along with the use of HCAT resulted in an increase in; density, asphaltene content, asphaltene density, and the softening point of the unconverted hydrocracked vacuum residue (H-Oil VTB). Using the data from Table 3 and from Table 5 and employing eq. 2 the following conversions of the C_5-, and C_7-asphaltenes before and after the application of HCAT were obtained:

	No HCAT	With HCAT
C_5-asphaltene conversion, wt.%	63.0	68.7
C_7-asphaltene conversion, wt.%	71.0	67.6

This data does not imply a change of the asphaltene conversion as a result of the use of HCAT in the LNB H-Oil VRO hydrocracker. This confirms data collected in the Pilot study which showed a plateau in asphaltene conversion (~70%) even as residue conversion continued to increase.

Considering the same asphaltene conversion with the use of the HCAT the reduction of the H-Oil VTB yield due to the higher VRO conversion inevitably is associated with a concentration increase of the asphaltenes and the resulting increase of the softening point of the VTB. It should be pointed out here that the total asphaltene conversion does not always give a notion about the changes occurring in the asphaltenes. For example, the most reactive asphaltene fraction in the residue hydroprocessing is the most soluble one [24]. The ratio between the asphaltene fractions having different solubility was shown by Rogel *et al*. [25] to affect the sedimentation during residue hydrocracking. Therefore, a deeper analysis of the asphaltene fractions is needed to explain the improvement of their solubility a result from the use of HCAT giving the opportunity to raise the ebullated bed vacuum residue hydrocracker reaction temperature and eventually to register a higher residue conversion.

Before the use of HCAT the softening point of the VTB was about 40°C. After the use of HCAT the softening point of the VTB raised up to about 60°C [26-27]. This change in the properties of the VTB at elevated residue conversion, will affect the recipes for production of road asphalt from feed blends containing H-Oil VTB. No change in the quality of the diesel after the use of HCAT was registered. Whereas the gas oils (HAGO, LVGO, and HVGO) demonstrated minor deterioration of the quality at elevated conversion with the use of HCAT. The Kw-characterization factor, established to characterize the quality of the H-Oil gas oils in our earlier research [27], showed that the HAGO Kw dropped from 11.40 down to 11.37; the LVGO Kw dropped from 11.26 down to 11.23; and the HVGO Kw dropped from 11.54 down to 11.46.

In order to evaluate the FCC unit performance with and without using HCAT at the LNB H-Oil VRO hydrocracker, the FCC performance for the dates 07.02.2020 (No use of HCAT), 15.02.2020 (HCAT in the H-Oil feed), and 09.03.2020 (HCAT in the H-Oil feed, but with increased content of FCC slurry in the H-Oil feed) is summarized in Table 6.

Table 6. LNB FCCU performance with and without using HCAT at the H-Oil hydrocracker.

Catalyst	Nad.975	Nad.975	Nad.975
Date	7.2.2020 (No HCAT)	15.2.2020 (With HCAT)	9.3.2020 (With HCAT)
FCC SLO in H-Oil feed, wt.%	7.8	8.3	14.2
FCC feed, t/h	237	231	237
FCC SLO Recycle, t/h	0	4	0
%H-Oil VGO in FCC feed	22	17	28
ROT, °C	538	538	538
CFT, °C	313	325	309
TRG dense, °C	688	688	689
TRG dilute, °C	700	700	702
CTO, wt./wt.	7.6	7.5	7.5
Yields on fresh feed basis, wt%			
C2 -	4.4	4.4	4.4
C3	8.2	9.2	7.5
C4	12.4	12.6	11.6
C5+ Gasoline	41.8	42.9	40.2
LCO	11.0	10.5	11.2
HCO	10.0	8.6	10.1
Slurry	8.0	7.5	10.5
Coke	4.4	4.4	4.5
Conversion	71.0	73.4	68.2
Corrected Conversion to FBP of 195°C	71.6	73.4	68.2
Corrected gasoline yield to FBP of 195°C	42.4	42.9	40.2
Corrected LCO yield to FBP of 195°C	10.4	10.5	11.2
FCC gasoline density at 15 °C, kg/m3	740	740	743
IBP, °C	34.2	34.8	37
10%, °C	50.3	51.4	53
50%, °C	86.9	88.3	91
90%, °C	162.5	164.6	166
FBP, °C	191.4	195.1	197
RON	94.4	93.8	94
MON	82.1	82	82
RVP, kPa	55.8	55.6	51.6
LCO density at 15 °C, kg/m3	919.4	923.7	924.4
IBP, °C	188	186	200
10%, °C	210	218	214
50%, °C	234	235	243
90%, °C	267	269	275
FBP, °C	296	298	307

The first impression is that the content of H-Oil VGO is different for the three studied dates (22% for the date 07.02.2020; 17% for the date 15.02.2020; and 28% for the date 09.03.2020). We found out in our earlier research that the content of H-Oil VGO has an impact on the LNB FCC unit performance [28]. Increasing H-Oil VGO content in the LNB FCC unit feed decreases the FCC conversion. If we use the regression developed earlier in the study [29] where it was shown that at each 1% variation of the H-Oil VGO content the FCC conversion may vary by 0.3% the difference in the corrected conversions between the dates 07.02.2020 and 15.02.2020 would have become 0.6%. This difference is within the uncertainty of defining of the LNB FCCU conversion for operation at the same conditions (0.8% is the uncertainty of the measurement of the conversion in the LNB FCCU [29]). Therefore, we cannot conclude that the quality of the H-Oil VGO after the use of HCAT has deteriorated to such an extent to affect considerably the LNB FCCU performance. If we take a look at the data on 09.03.2020 we can see a considerable drop in the LNB FCCU conversion, a result from the increased share of H-Oil VGO in the FCC feed (28%) and worsened quality of the H-Oil VGO as can be seen from the data in Table 5 for this date. All these factors contributed to a conversion decrease in amount of about 3-4%. The reduction of the FCC SLO content in the H-Oil feed should be considered especially after the use of HCAT catalyst that has been demonstrated to decrease sediment formation in the H-Oil ebullated bed VRO hydrocracking.

4. Conclusions

The application of the nano-size HCAT catalyst significantly reduced ATB sediment formation in both Pilot testing and subsequent commercial application at the LNB H-Oil VRO hydrocracker. The efficacy of the HCAT Technology was exhibited while processing a 70% Urals/30% Middle East crude feed blend, along with a commercial Ni-Mo supported catalyst. Due to the reduced rate of sediment formation during the use of HCAT, the WABT could be increased and enhanced conversion can be registered. At LNB, the approximate 8 W% increase in residue conversion resulted in higher yields of gas, naphtha, and diesel. The low value heavy oil products, unconverted hydrocracked vacuum residue, and VGO showed decline in their yields after implementation of the HCAT technology in both laboratory pilot plant and commercial LNB H-Oil VRO hydrocrackers. The conversion of the asphaltenes showed no improvement and as a result due to the concentration of the asphaltenes in the VTB after the use of HCAT the VTB softening point was raised. This will have impact on the recipes for production of road asphalt from feed blends containing H-Oil VTB. The H-Oil diesel quality is not affected by the use of HCAT, while the H-Oil VGO quality showed minor signs of possible deterioration at elevated residue conversion. The performance of the LNB FCCU was not measurably impacted as a result of the changes in the H-Oil VGO quality during HCAT usage. Increasing the FCC SLO share in the H-Oil feed does not have a beneficial effect on the sediment formation rate reduction in H-Oil unit but does have a negative impact on the FCCU performance. Therefore, reconsidering of the use of FCC SLO in the LNB H-Oil should be made, especially after the application of the nano-size HCAT catalyst.

References

[1] Bannayan MA. Lemke, H. K.; Stephenson, W. K. Fouling mechanisms and effect of process conditions on deposit formation in H-Oil. Studies in Surface Science and Catalysis, 1996; 100: 273-281.

[2] Pang WW, Kuramae M, Kinoshita Y, Lee JK, Zhang YZ, Yoon SH, Mochida I. Plugging problems observed in severe hydrocracking of vacuum residue. Fuel, 2009; 88: 663–669.

[3] García FO, Mar-Juárez E, Hernández PS. Controlling Sediments in the Ebullated Bed Hydrocracking Process. Energy & Fuels, 2012, 26: 2948−2952.

[4] Stanislaus A, Hauser A, Marafi M. Investigation of the mechanism of sediment formation in residual oil hydrocracking process through characterization of sediment deposits. Catal. Today, 2005; 109: 167–177.

[5] Stratiev D, Shishkova I, Nikolaychuk E, Dinkov R, Stoilov G, Yankov V, Mitkova M. Impact of severity in the H-Oil vacuum residue hydrocracking on sediment formation. Pet Coal, 2019; 61(5): 1166-1182.

[6] Marques J, Maget, S, Verstraete JJ. Improvement of Ebullated-Bed Effluent Stability at High Conversion Operation. Energy & Fuels, 2011; 25: 3867–3874.
[7] Stratiev D, Shishkova I, Nikolaychuk E, Anastasov M, Stanulov K, Toteva V. Effect of catalyst condition on sedimentation and conversion in the ebullated bed vacuum residue H-Oil hydrocracking. Pet. Sci. Technol., 2019; 37 (12): 1463-1470.
[8] Gragnani A ,Putek S. Resid hydrocracker produces low-sulfur diesel from difficult feeds. Hydrocarbon Processing, May 2006; 85: 95–100.
[9] Lakhanpal B, Klein D, Leung P, Tombolesi B, Kubiak J. Upgrading heavy oils with new catalyst technology. Petroleum Technology Quarterly, Autumn 2004, 41–47.
[10] Stratiev D, Shishkova I, Nikolaychuk E, Ilchev I, Yordanov D. Investigation of the Effect of Severity Mode of Operation in the H-Oil Vacuum Residue Hydrocracking on Sediment Formation During Processing Different Feeds. Pet Coal, 2020; 62(1) 50-62.
[11] Respin M, Ekres S, Wright B, Žajdlík R. Strategies to control sediment and coke in a hydrocracker. PTQ Q2 2013, www.digitalrefining.com/article/1000794.
[12] Chabot J, Shiflett W. Residuum hydrocracking: chemistry and catalysis, PTQ Q3 2019, www.digitalrefining.com/article/1002340.
[13] Bellussi G, Rispoli G, Landoni A, Millini R, Molinari D, Montanari E, Moscotti D, Pollesel P. Hydroconversion of heavy residues in slurry reactors: Developments and perspective. Journal of Catalysis. 2013; 308: 189-200.
[14] Kunnas J, Smith L. Improving residue hydrocracking performance, PTQ Q3, 2011.
[15] Silverman B, Sláva J, Gendler J. The HCAT® Technology at Slovnaft A Year in Review, BBTC 2016, 12th to 13th May 2016, Madrid, Spain.
[16] US patent. Upgraded ebullated bed reactor with increased production rate of converted products. US-20170081599-A1. (2017). https://app.dimensions.ai/details/patent/US-20170081599-A1
[17] Tye CT. Catalysts for Hydroprocessing of Heavy Oils and Petroleum Residues, 2019, Open access peer-reviewed chapter, https://www.intechopen.com/books/processing-of-heavy-crude-oils-challenges-and-opportunities/catalysts-for-hydroprocessing-of-heavy-oils-and-petroleum-residues.
[18] Stratiev D, Dinkov R, Shishkova I, Sharafutdinov I, Ivanova N, Mitkova M, Yordanov D, Rudnev N, Stanulov K. What is behind the high values of hot filtration test of the ebullated bed residue H-Oil hydrocracker residual oils. Energy & Fuels, 2016. 2016; 30(9): 7037-7054.
[19] IP 375: Petroleum products - Total sediment in residual fuel oils - Part 1: Determination by hot filtration.
[20] IP 390: Petroleum products - Total sediment in residual fuel oils - Part 2: Determination using standard procedures for ageing
[21] Stratiev D, Shishkova I, Nikolaychuk E, Ijlstra W, Holmes B, Caillot M. Feed Properties Effect on the Performance of Vacuum Residue Ebullated Bed H-Oil Hydrocracking. OGEM, 2019; 4: 194-199.
[22] Stratiev D, Shishkova I, Dinkov R, Yordanov D. Studying of the processing of fluid catalytic cracking slurry oil in the H-Oil ebullated bed vacuum residue hydrocracking and its effect on the H-Oil vacuum gas oil quality and fluid catalytic cracking performance, Pet Coal, 2020; 62(2): 542-556.
[23] Stratiev D, Shishkova I, Dinkov R, Kolev I, Ivanov E, Yankov V, Yordanov D, McNamara D. Petroleum crude slate effect on H-Oil performance. Int. J. Oil, Gas and Coal Technology, 2021; 28 (3): 259 - 286.
[24] Ovalles C, Rogel E, Moir M, Brait A. Hydroprocessing of Vacuum Residues. Asphaltene Characterization and Solvent Extraction of Spent Slurry Catalysts and the Relationships with Catalyst Deactivation. Applied Catalysis A General, 2016; 532: 57-64 .
[25] Rogel E, Ovalles C, Pradhan A. Sediment Formation in Residue Hydroconversion Processes and Its Correlation to Asphaltene Behavior. Energy & Fuels, 2013; 27: 6587−6593.
[26] Stratiev D, Shishkova I, Dinkov R, Kirilov K, Yordanov D, Nikolova R, Veli A, Tavlieva M, Vasilev S, Suyunov R. Variation of oxidation reactivity of straight run and H-Oil hydrocracked vacuum residual oils in the process of road asphalt production. Road Materials and Pavement Design, DOI: 10.1080/14680629.2021.1893209.
[27] Dinkov R, Stratiev D, Shishkova I, Yordanov D, Nikolova R, Veli A, Ilchev I. Opportunity to increase the share of unconverted vacuum tower bottom from residue hydrocracking (H-Oil) in paving grade bitumen production. Oxidation Communications, 2020; 43(2): 302-320.

[28] Stratiev D, Shishkova I, Ivanov M, Chavdarov I, Yordanov D. Dependence of Fluid Catalytic Cracking Unit Performance on H-Oil Severity, Catalyst Activity, and Coke Selectivity. Chemical Technology and Engineering, 2020; 43(11): 2266-2276.
[29] Stratiev D, Shishkova I, Petrov I, Yordanov D, Toteva V. Petroleum crude slate, catalyst properties and H-Oil VGO properties effects on a commercial FCC unit performance, Journal of Chemical Technology and metallurgy, 2021, 56(3): 488-498.

To whom correspondence should be addressed: professor DSc Dicho Stratiev, LUKOIL Neftohim Burgas, 8104 Burgas, Bulgaria, E-mail: *Stratiev.Dicho@neftochim.bg*